Research Square

Preprints are preliminary reports that have not undergone peer review.
They should not be considered conclusive, used to inform clinical practice,
or referenced by the media as validated information.

Evidence for persistent net heterotrophy in blackwater estuaries and the importance of depth-resolved community respiration measurements

Mingying Chuo

mchuo@unc.edu

University of North Carolina at Chapel Hill

Nathan Hall

University of North Carolina at Chapel Hill

Article

Keywords: Blackwater estuary, primary production, community respiration, net community production, heterotrophy

Posted Date: November 20th, 2026

DOI: https://doi.org/10.21203/rs.3.rs-11637788/v1

License: This work is licensed under a Creative Commons Attribution 4.0 International License.
Read Full License

Additional Declarations: No competing interests reported.

Evidence for persistent net heterotrophy in blackwater estuaries and the importance of depth-resolved community respiration measurements

Mingying Chuo*, Nathan S. Hall

Department of Earth, Marine and Environmental Sciences, Institute of Marine Sciences, University of North Carolina at Chapel Hill, Morehead City, North Carolina, USA

Corresponding author: Mingying Chuo (mchuo@unc.edu)

Abstract

Blackwater estuaries receive large quantities of terrestrial organic carbon, yet the extent to which this carbon is consumed through estuarine respiration remains poorly constrained. Here, we investigate seasonal and vertical variability in blackwater estuary pelagic metabolism. Both depth-integrated gross primary production (GPP) and community respiration (CR) exhibit pronounced seasonality, with elevated rates during warmer months. CR generally declines with depth. Neglecting vertical variability in CR substantially biases estimates of depth-integrated CR and net community production (NCP). The pelagic community is net heterotrophic (negative depth-integrated NCP) throughout the study period. Net heterotrophy is strongest in summer. These findings show that blackwater estuaries can exhibit persistent pelagic net heterotrophy, suggesting that substantial organic carbon may be processed through pelagic respiration. The observed vertical variability in CR underscores the importance of depth-resolved measurements for accurately quantifying this carbon transformation.

Keywords: Blackwater estuary; primary production; community respiration; net community production; heterotrophy

Introduction

Blackwater estuaries and their upstream watersheds are characterized by darkly stained waters resulting from high concentrations of colored dissolved organic matter (CDOM), primarily derived from the decomposition of terrestrial vegetation in surrounding forests, wetlands, and peatlands[1]. These systems represent some of the most carbon-rich aquatic environments, with dissolved organic carbon (DOC) yields that can reach up to 30 times the global average for large rivers[2,3]. Despite their potentially substantial DOC export, blackwater systems remain underrepresented in assessments of aquatic carbon cycling[4]. Understanding the fate of terrestrial carbon within

blackwater estuaries is therefore critical for assessing the contributions of these systems to regional and global carbon budgets.

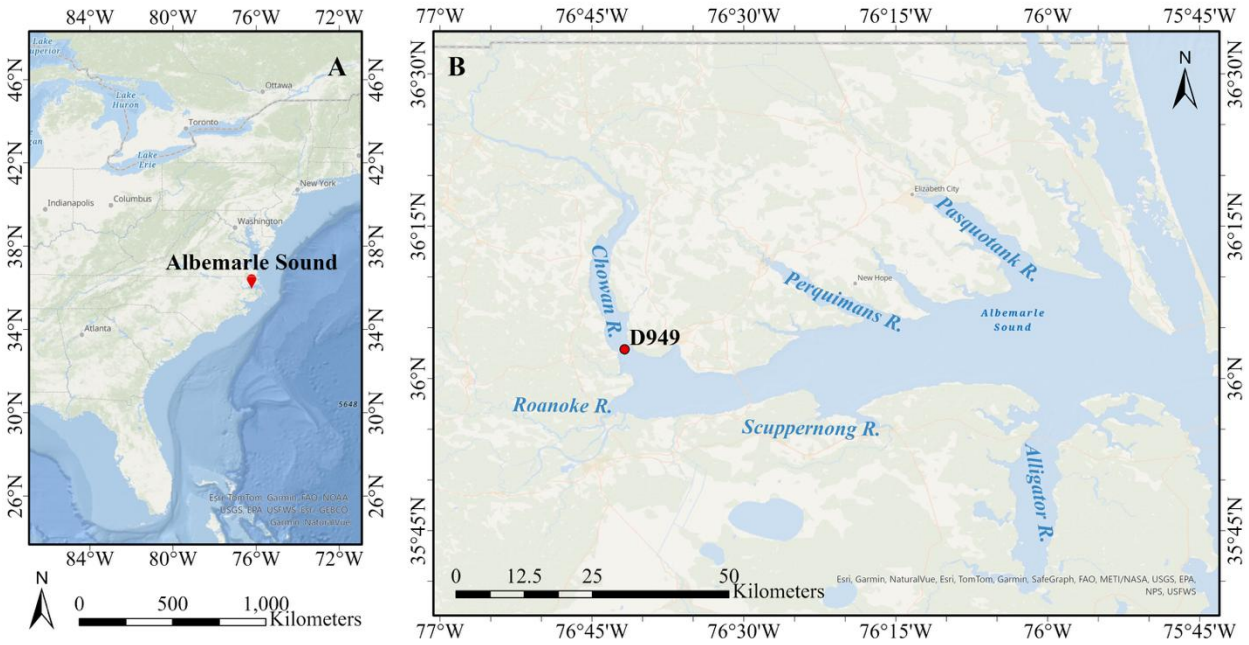
High DOC concentrations can strongly influence ecosystem metabolism in blackwater systems. Terrestrially derived organic matter provides an abundant substrate for microbial respiration, whereas elevated concentrations of CDOM reduce light penetration and limit phytoplankton photosynthesis[5]. Consequently, community respiration (CR) often exceeds gross primary production (GPP). The balance between GPP and CR is quantified as net community production (NCP), defined as GPP minus CR[6]. Positive NCP indicates net autotrophy, whereas negative NCP indicates net heterotrophy.

Variations in environmental conditions among estuaries can alter the relative magnitudes of GPP and CR, contributing to differences in whether systems are autotrophic or heterotrophic. Greater light availability and warmer temperatures during summer can enhance GPP and, when GPP exceeds CR, shift the system toward net autotrophy[7,8]. In DOC-rich systems, however, abundant organic carbon may stimulate CR sufficiently to offset increases in GPP and maintain net heterotrophy[9]. Quantifying the variability of GPP and CR in blackwater estuaries is essential for determining whether these systems are net autotrophic or heterotrophic, and for understanding how estuarine metabolism processes terrestrial carbon before its export to downstream coastal waters.

The Atlantic Coastal Plain of the eastern United States contains extensive networks of blackwater rivers, which account for 18.2% of the region's river length[10]. The Chowan River, a DOC-rich blackwater estuary in northeastern North Carolina (Fig. 1), provides an ideal system for investigating pelagic carbon metabolism. Extensive wetlands and forested landscapes within its watershed sustain high DOC concentrations[1], while seasonal phytoplankton blooms[11,12],

53 particularly in downstream reaches, contribute additional autochthonous organic matter that may
54 stimulate microbial respiration[13]. Its long, ~ 50-day residence time[14] further promotes biological
55 transformation of both terrestrial and autochthonous organic carbon.

56 Despite the importance of blackwater estuaries in transforming terrestrially derived organic carbon,
57 seasonal and vertical variability in pelagic metabolism remains poorly characterized. In particular,
58 to our knowledge, no previous studies have simultaneously quantified GPP and CR across multiple
59 depths and seasons in blackwater estuaries. Here, we investigated pelagic metabolism in the
60 Chowan River over a two-year period to quantify seasonal and vertical variability in GPP and CR
61 and determine whether the water column is net autotrophic or net heterotrophic. We hypothesized
62 that high DOC availability and reduced light penetration would result in persistent net heterotrophy
63 by stimulating CR relative to GPP.



64

65 **Fig. 1.** Map of the Albemarle Sound system, showing the location of Albemarle Sound in the
66 United States (A) and the study site in the Chowan River (B).

Results

Environmental and biogeochemical setting

During the 2023-2025 study period, water temperature exhibited a pronounced seasonal cycle, ranging from 2.7 to 31.3 °C, with the highest values occurring during summer and the lowest during winter (Fig. 2a). In contrast, the vertical light attenuation coefficient remained consistently high throughout the study, ranging from 1.0 to 2.9 m^{-1} (Fig. 2b).

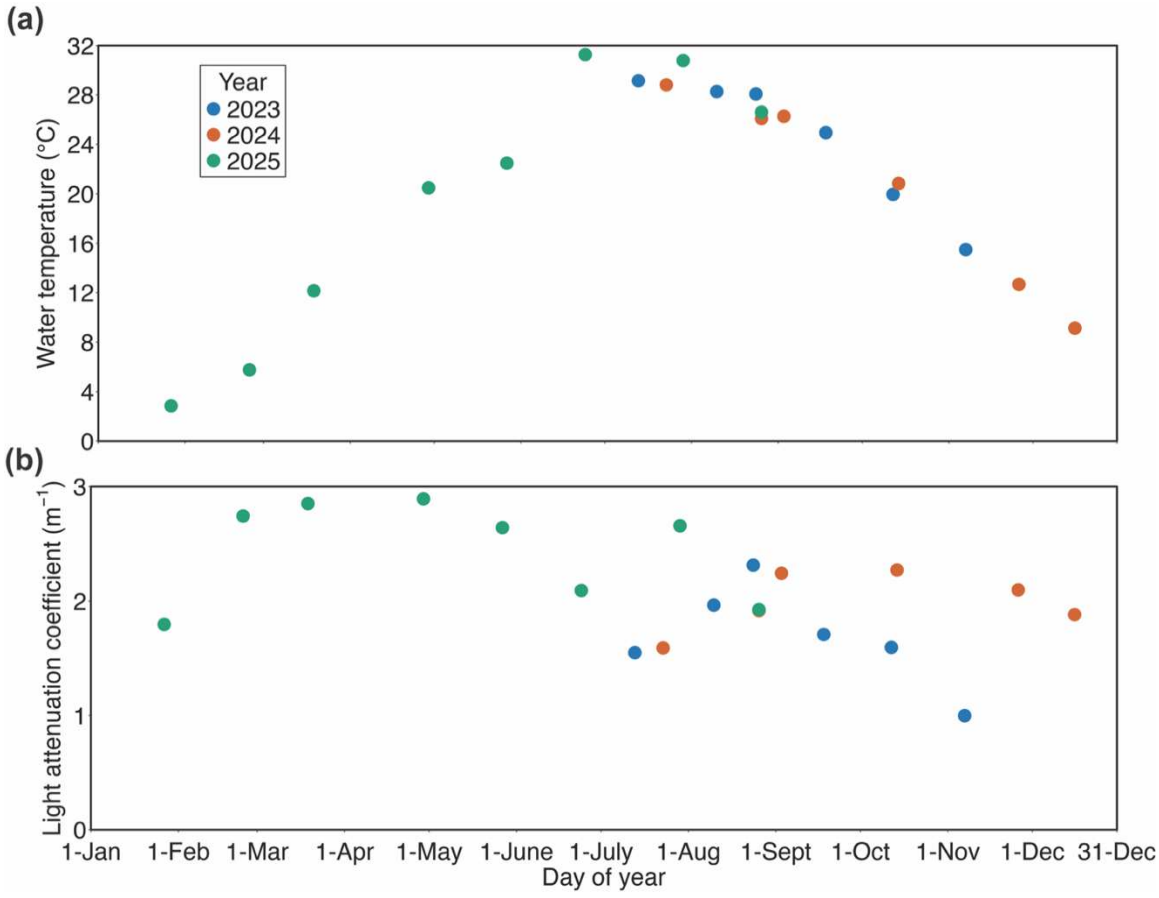


Fig. 2. Seasonal variation in (a) surface water temperature and (b) vertical light attenuation coefficient in the Chowan River during the study period. Sampling years are distinguished by point color.

Chlorophyll *a* concentrations ranged from 0.6 to 18.0 µg L^{-1} (median 5.1 µg L^{-1}), with generally higher concentrations during summer (Fig. 3a). Chlorophyll *a* showed limited vertical variation, with no significant difference between surface and Secchi depth. Concentrations at twice the Secchi depth were generally similar to or lower than those at shallower depths.

DOC concentrations remained consistently high throughout the study, ranging from 512 to 1,113 µmol L^{-1} (median 858 µmol L^{-1}), with little variation between sampling depths (Fig. 3b). DIN concentrations ranged from 1.0 to 16.2 µmol L^{-1} (median 3.5 µmol L^{-1}), with lower concentrations during summer (Fig. 3c). DIP concentrations ranged from 0.1 to 4.5 µmol L^{-1} (median 0.5 µmol L^{-1}), with relatively little seasonal variation (Fig. 3d).

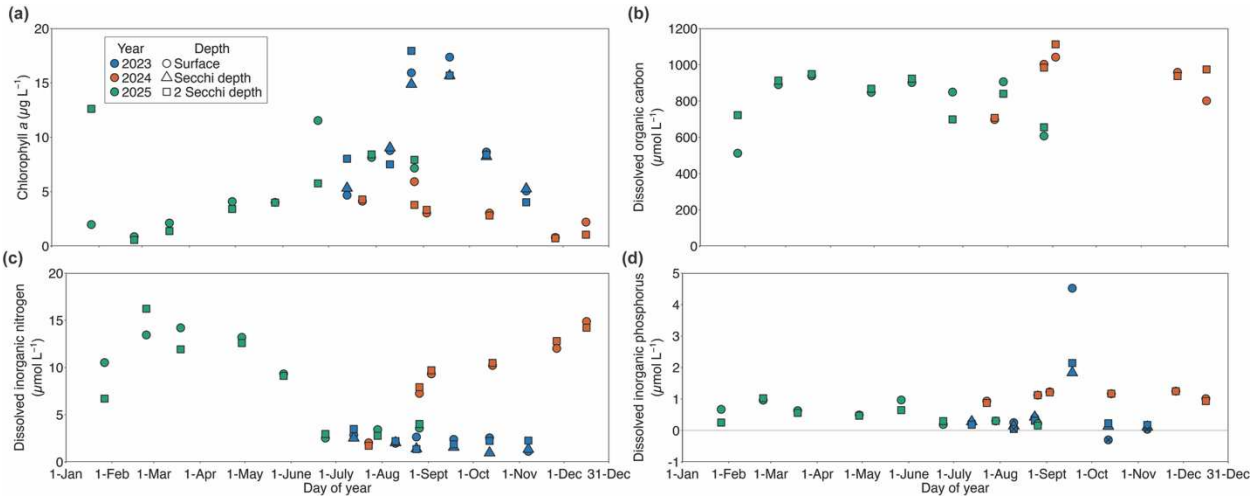


Fig. 3. Seasonal and vertical variation in (a) chlorophyll *a*, (b) dissolved organic carbon (DOC), (c) dissolved inorganic nitrogen (DIN), and (d) dissolved inorganic phosphorus (DIP) at the surface, Secchi depth, and twice the Secchi depth in the Chowan River during the study period. Samples from the Secchi depth were collected in 2023; thereafter, only surface and twice the Secchi depth were sampled. Sampling years are distinguished by symbol color, and sampling depths are

distinguished by symbol shape. For DIP, measurements below the detection limit are indicated by an "X" within the corresponding symbol.

Seasonal variability in primary production

Depth-integrated GPP ranged from 0 to 68 mmol O_2 m^{-2} d^{-1} (median 13 mmol O_2 m^{-2} d^{-1}) and showed pronounced seasonal variation (Fig. 4). Depth-integrated GPP was significantly higher in summer than winter, following seasonal changes in temperature and solar radiation. Higher depth-integrated GPP during summer also coincided with increases in phytoplankton biomass (Fig. 3a).

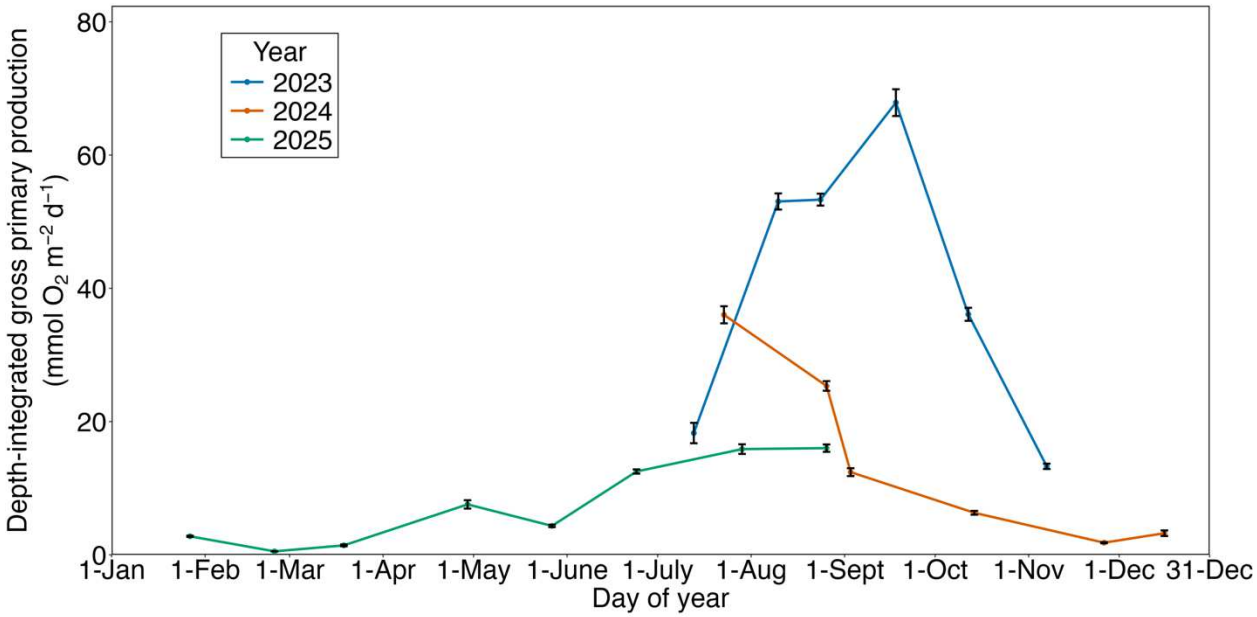


Fig. 4. Seasonal variation in depth-integrated gross primary production (GPP) in the Chowan River during the study period. Sampling years are distinguished by line color. Error bars represent the standard deviation of the integrated GPP bootstrap distribution.

Seasonal and vertical variability in community respiration

The measured CR showed significant seasonal variation, driven primarily by higher rates in summer than winter (Fig. 5). CR decreased significantly with increasing depth, with respiration rates at the surface higher than those at twice the Secchi depth.

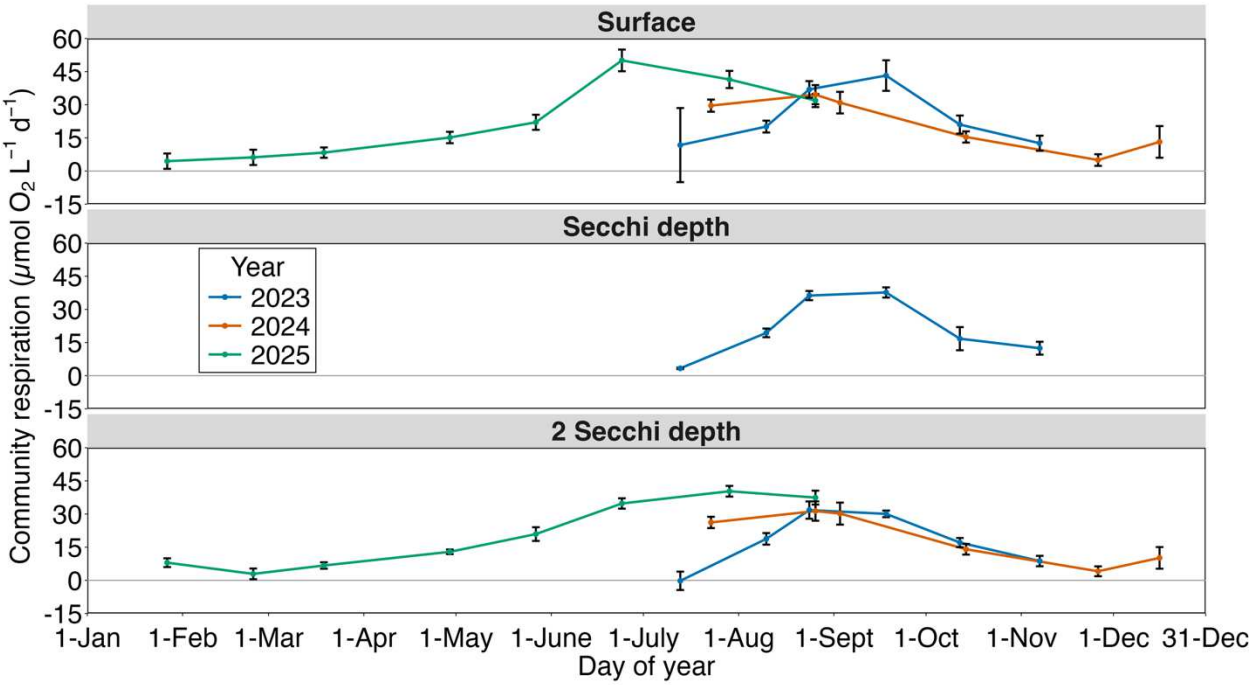


Fig. 5. Seasonal and vertical variation in pelagic community respiration (CR) in the Chowan River during the study period. Samples from the Secchi depth were collected in 2023; thereafter, only surface and twice the Secchi depth were sampled. Sampling years are distinguished by line color. Bars are the mean and error bars are standard deviations.

Depth-integrated CR ranged from 5 to 259 mmol O_2 m^{-2} d^{-1} (median 120 mmol O_2 m^{-2} d^{-1}) and varied significantly among seasons (Fig. 6). Higher depth-integrated CR was observed during the summer months. In contrast, depth-integrated CR was substantially lower during winter, with values generally below 50 mmol O_2 m^{-2} d^{-1}.

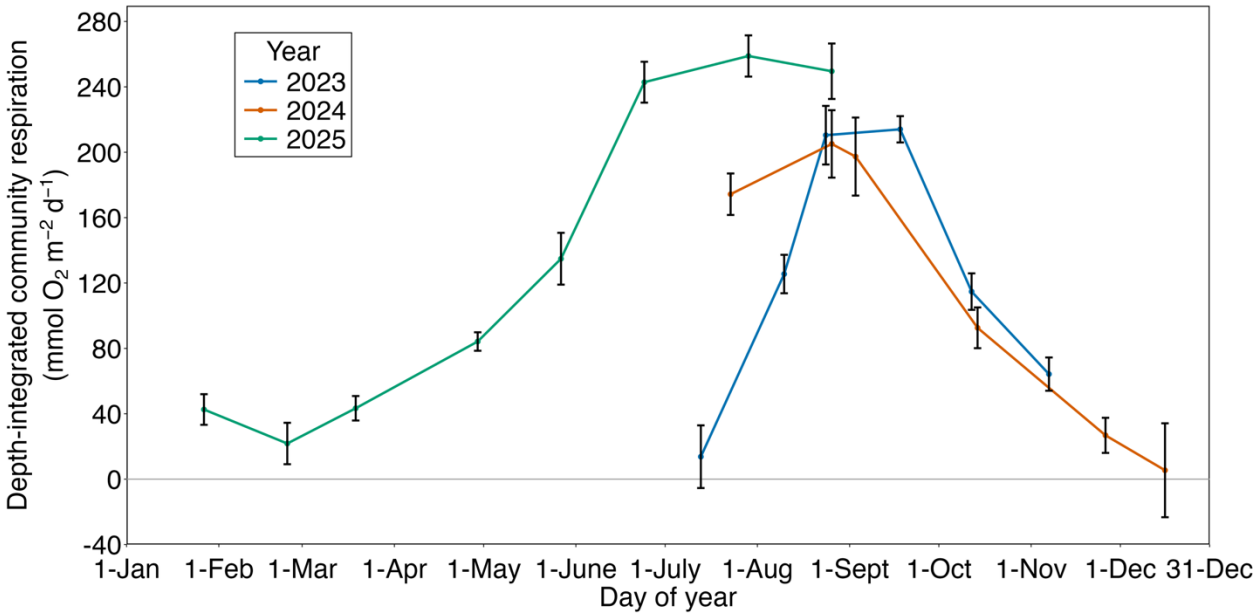


Fig. 6. Seasonal variation in depth-integrated community respiration (CR) in the Chowan River during the study period. Sampling years are distinguished by line color. Error bars represent 95% confidence intervals for depth-integrated CR calculated from uncertainty propagated from the standard errors of the measured CR estimates.

Additionally, we compared depth-integrated CR calculated from the observed vertical profiles (Fig. 6) with estimates obtained by assuming that surface CR remained constant throughout the water column. Assuming CR was constant with depth and equal to the surface CR resulted in higher depth-integrated CR estimates in 90% of sampling cases (18 of 20), whereas estimates were lower in the remaining 10% (2 of 20). Among the 18 overestimation cases, the assumption resulted in a mean overestimation of 23 mmol O_2 m^{-2} d^{-1} (median 15), corresponding to a mean percent difference of 57% (median 16%) relative to estimates based on the observed vertical CR profiles (Table 1). The magnitude of the discrepancy varied substantially among dates, with particularly large relative differences occurring when depth-integrated CR was low.

Table 1

Comparison of depth-integrated community respiration (CR) calculated from observed vertical CR profiles ("Observed") and calculated by assuming that CR remained constant with depth at the surface CR value ("Assumed"). Depth-integrated CR was in unit mmol O_2 m^{-2} d^{-1}.

Sampling date	Observed	Assumed	Difference	Percent difference (%)
13-July-2023	13.7	77.5	63.7	464.0
10-August-2023	125.5	132.8	7.3	5.8
24-August-2023	210.4	236.5	26.1	12.4
18-September-2023	214.0	285.1	71.1	33.2
12-October-2023	114.7	138.7	24.0	20.9
7-November-2023	64.3	80.4	16.2	25.2
23-July-2024	174.3	192.4	18.0	10.3
26-August-2024	205.1	221.2	16.1	7.9
3-September-2024	197.4	201.2	3.8	1.9
14-October-2024	92.6	100.2	7.6	8.2
26-November-2024	26.8	31.3	4.5	16.8
16-December-2024	5.4	19.3	13.9	256.2
27-January-2025	42.6	26.8	-15.8	-37.1
24-February-2025	21.8	40.2	18.4	84.3
19-March-2025	43.4	52.5	9.1	21.0
29-April-2025	84.2	97.1	12.9	15.3
27-May-2025	134.9	141.2	6.3	4.7
24-June-2025	242.9	325.4	82.6	34.0
29-July-2025	258.9	265.2	6.3	2.4
26-August-2025	249.6	216.9	-32.6	-13.1

Mean (all dates)	126.1	144.1	18.0	48.7
Median (all dates)	120.1	135.7	13.4	13.8
Mean (overestimation cases)	123.9	146.6	22.7	56.9
Median (overestimation cases)	120.1	135.7	15.0	16.0

Seasonal variability in net community production

Depth-integrated NCP was negative on all but one sampling date, ranging from -243 to -2 mmol O_2 m^{-2} d^{-1} (median -86 mmol O_2 m^{-2} d^{-1}; Fig. 7). The single positive NCP value had an uncertainty interval that overlapped zero, providing no clear evidence of net autotrophy. Overall, the Chowan River exhibited persistent pelagic net heterotrophy. The magnitude of net heterotrophy varied significantly among seasons, with more negative NCP values occurring during summer and less negative values during winter (Fig. 7).

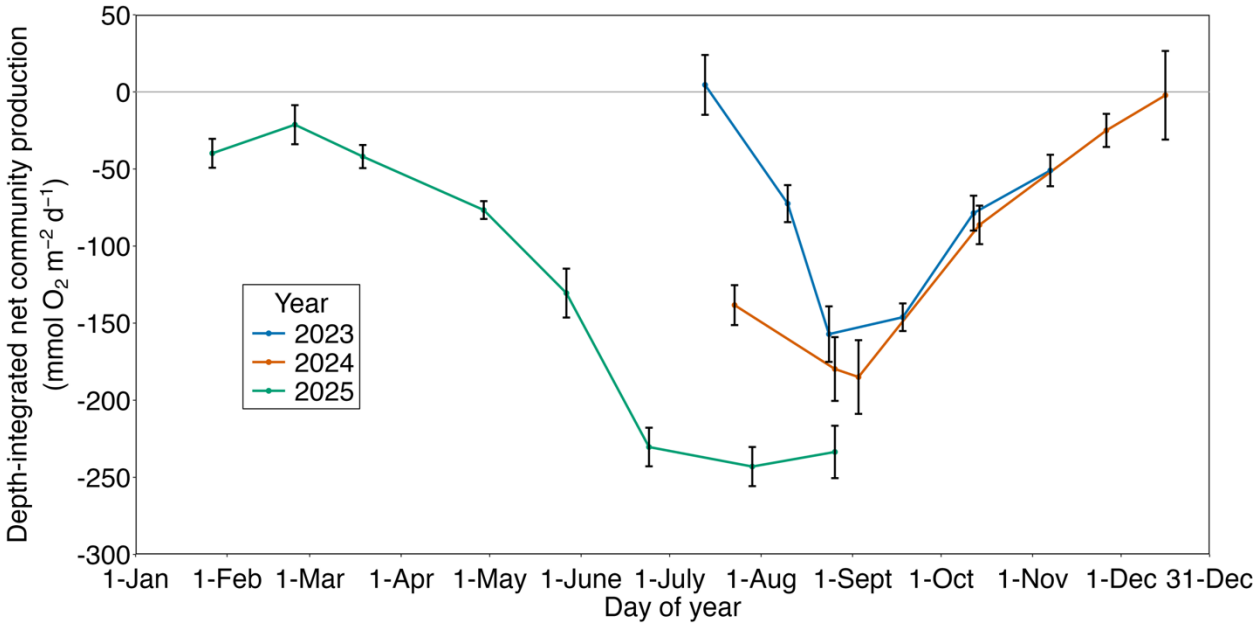


Fig. 7. Seasonal variation in depth-integrated pelagic net community production (NCP) in the Chowan River during the study period. Negative values indicate net heterotrophy, whereas positive values indicate net autotrophy. Sampling years are distinguished by line color. Error bars represent 95% uncertainty intervals based on propagated uncertainties in GPP and CR.

Discussion

Depth-integrated pelagic NCP remained negative throughout the two-year study period, indicating persistent pelagic net heterotrophy in the Chowan River. The mean NCP observed in this study (-107 mmol O_2 m^{-2} d^{-1}) was more negative than the mean values (-67 mmol O_2 m^{-2} d^{-1}) reported for a collection of 45 temperate, subtropical, and tropical estuaries[7,15,16]. Furthermore, the lowest observed NCP (-243 mmol O_2 m^{-2} d^{-1}) was approximately 5-21 times more negative than the reported minima in recent studies[16,17], highlighting the exceptionally strong pelagic heterotrophy of this blackwater estuary. Strong heterotrophic carbon processing has also been documented in other southeastern U.S. rivers and estuaries, where high rates of respiration and terrestrial organic carbon processing contribute to substantial CO_2 production and outgassing[18-20]. Persistent pelagic heterotrophy has likewise been reported in some other DOC-rich rivers and estuaries, where abundant terrestrial organic matter and limited light availability favor respiration over primary production[5,21]. Our results extend these observations by demonstrating consistently negative depth-integrated pelagic NCP across seasons in a blackwater estuary system of the U.S. Atlantic Coastal Plain, based on direct measurements of depth-resolved GPP and CR.

The persistent pelagic net heterotrophy observed in the Chowan River likely reflects the combination of elevated DOC concentrations and strong light attenuation. DOC concentrations remained high throughout the study, consistent with substantial terrestrial carbon inputs characteristic of blackwater systems[1,3]. Additionally, the consistently high light attenuation coefficients indicated limited light penetration through the water column, restricting phytoplankton GPP largely to surface waters. Consequently, although phytoplankton biomass and GPP increased during summer, the increase in depth-integrated GPP was relatively small because production was concentrated within the shallow euphotic zone. In contrast, CR extended throughout the water

column, resulting in depth-integrated CR consistently exceeding depth-integrated GPP and yielding persistent negative pelagic NCP.

The magnitude of pelagic heterotrophy exhibited strong seasonal variation, with the most negative NCP values occurring during summer. This pattern coincided with higher CR during the warm season. Temperature is a primary regulator of aquatic respiration; higher temperatures accelerate microbial metabolic activity and the rate of organic matter degradation[22]. In the Chowan River, elevated summer temperatures likely supported greater respiratory activity and widened the difference between depth-integrated CR and GPP.

Many water-column metabolism studies assume vertically uniform respiration because measurements are frequently limited to surface waters[23,24]. Such an assumption may be more appropriate in strongly tidal and well-mixed estuaries, where physical mixing can reduce vertical gradients in metabolic rates[18,19,25]. In contrast, we found that CR exhibited clear vertical variability in the Chowan River. CR at twice the Secchi depth was, on average, approximately 16% lower than at the surface, although the magnitude of this difference varied among dates. The assumption of vertically uniform CR resulted in an overestimation of depth-integrated CR compared with estimates calculated from the observed vertical profiles. Therefore, neglecting vertical variability in CR can bias estimates of depth-integrated CR and, consequently, pelagic NCP.

Because water temperature varied little with depth, the lower CR at depth was unlikely to be driven by temperature differences. Instead, the vertical pattern may reflect differences in the availability of organic carbon substrates. Estuarine respiration can be supported by both allochthonous organic matter from terrestrial and marsh sources and autochthonous organic matter produced within the estuary, with their relative contributions varying among systems[7,22]. In the Chowan River, high

192 levels of terrestrially derived DOC provide an important allochthonous carbon source for
193 respiration[1], while strong light attenuation restricts autochthonous production largely to surface
194 waters. The lower CR at depth may therefore reflect reduced availability of recently produced,
195 readily respired organic substrates below the productive surface layer, although the relative
196 contributions of allochthonous and autochthonous carbon were not directly quantified in this study.

197 This study focused on a single site in the lower reach of the Chowan River. This might raise the
198 question of whether the patterns observed at this specific location were representative of the
199 Chowan River as a whole. As previously discussed, the persistent pelagic net heterotrophy
200 observed in the Chowan River was likely driven by high DOC concentrations and strong light
201 attenuation. DOC concentrations and light attenuation in the upstream reaches of the Chowan
202 River were comparable to, or even higher than those observed at the downstream sampling site in
203 this study[1,26]. Furthermore, chromophoric dissolved organic matter varied primarily over time
204 rather than space[1]. However, during downstream transport, chromophoric dissolved organic matter
205 was likely to decrease due to photobleaching or microbial degradation[27], resulting in lower
206 concentrations downstream and, consequently, reduced absorption of sunlight by the
207 chromophoric dissolved organic matter. In addition to DOC concentrations and chromophoric
208 dissolved organic matter, water temperature and concentrations of nitrogen and phosphorus did
209 not vary much across different sections of the Chowan River[14]. Therefore, higher DOC
210 concentrations, stronger light attenuation, and possibly higher chromophoric dissolved organic
211 matter may have caused upstream waters to be more heterotrophic than downstream waters. We
212 can expect this net heterotrophic characteristic to reflect the overall condition of the entire river.

213 Unlike many temperate estuaries that exhibit seasonal shifts between net autotrophy and
214 heterotrophy[8], the persistent net heterotrophy in the Chowan River suggests that blackwater

estuaries may function as more important sites for the transformation of terrestrial organic carbon before its export to downstream coastal waters. Because blackwater rivers are widespread across many coastal regions yet remain underrepresented in metabolic studies[4], incorporating pelagic metabolism measurements from these systems into regional and global assessments could better constrain the role of blackwater estuaries in carbon cycling across the land-ocean aquatic continuum. By resolving both seasonal and vertical variability in production and respiration, this study demonstrates the importance of accounting for these sources of variability when assessing carbon processing in blackwater estuaries. Integrating pelagic metabolism with benthic processes and direct carbon flux measurements would provide a more complete assessment of the role of blackwater systems in regional and global carbon cycling.

Methods

Sample collection

Field sampling was conducted monthly during the early morning (~07:00) from July 2023 to August 2025 at Station D949 in the Chowan River (Fig. 1). Vertical profiles of water temperature, salinity, turbidity, dissolved oxygen, conductivity and pH were measured using a YSI 6600 multiparameter sonde. Photosynthetically active radiation profiles were measured with a Li-Cor Li-192 underwater quantum sensor to estimate the vertical light attenuation coefficient. Measurements of Secchi depth were performed on the sunlit side of the boat, and the euphotic depth was estimated as twice the Secchi depth[28].

To quantify pelagic metabolism within the euphotic zone, 2 L water samples were collected from the surface, the Secchi depth and twice the Secchi depth in 2023. Preliminary analyses indicated that GPP and CR were similar between the surface and the Secchi depth. Consequently, from May 2024 onward, samples were collected only from the surface and twice the Secchi depth. Water

samples were used for ^{14}C uptake experiments, CR measurements, and determination of nutrients, phytoplankton biomass, and phytoplankton community composition.

Nutrients and phytoplankton biomass

Dissolved inorganic nitrogen (DIN, NO_x (NO_3^- + NO_2^-) + NH_4^+) and dissolved inorganic phosphorus (DIP, i.e., PO_4^{3-}) and silicate (SiO_2) were determined according to Peierls et al. (2012)[29] on subsamples (40 mL) filtered through pre-combusted (4 hours at 550 °C) Whatman GF/F filters using standard colorimetric methods on a QuAAtro39 Continuous Segmented Flow Analyzer from SEAL analytical. The detection limit was 0.45 µmol L^{-1} for NO_x, 0.22 µmol L^{-1} for NH_4^+, 0.05 µmol L^{-1} for PO_4^{3-} and 1.83 µmol L^{-1} for SiO_2.

Dissolved organic carbon (DOC) was measured using a Shimadzu TOC-L Analyzer[30]. Water samples (40 mL) were filtered through pre-combusted (4 hours at 550 °C) Whatman GF/F filters. The filtrate was stored in pre-combusted glass scintillation vials with Teflon closures and frozen at -20 °C until analysis. The Shimadzu TOC-L Analyzer used high temperature catalytic oxidation followed by non-dispersive infrared analysis of the CO_2 produced. Samples were acidified to a pH less than 2 and sparged with air before they were analyzed for non-volatile organic carbon.

High performance liquid chromatography (HPLC) was used to determine chlorophyll *a* (Chla), a proxy for total phytoplankton biomass. Duplicate aliquots of 100 mL sample water were filtered onto Whatman GF/F filters which were subsequently extracted in 100% acetone, sonicated, and stored at 20 °C for approximately 24 hours prior to HPLC analysis[31].

^{14}C uptake experiments

Photosynthesis-irradiance relationships were determined from ^{14}C uptake using a temperature-controlled photosynthetron[32]. The radioactivity of the $NaH^{14}CO_3$ stock solution was determined

by mixing an aliquot of the stock solution with phenethylamine and Ecolume scintillation cocktail and measuring the activity by liquid scintillation counting. Water samples were amended with $NaH^{14}CO_3$ and dispensed into 24 scintillation vials. Three vials served as time-zero controls to quantify non-biological ^{14}C uptake, whereas the remaining 21 vials were incubated for 10 min under irradiances spanning approximately 0-2000 µE m^{-2} s^{-1}. Incubations were conducted at the in situ surface water temperature measured during sampling. At the end of each incubation, samples were acidified with 6 N HCl to terminate photosynthesis and remove unincorporated inorganic ^{14}C. Samples were left on a shaker overnight, neutralized with 6 N NaOH, mixed with Ecolume scintillation cocktail, and radioactivity was measured using a Beckman LS 6500 Scintillation Counter. Dissolved inorganic carbon concentrations were determined using the Shimadzu TOC-L Analyzer.

Photosynthesis-irradiance curves were fitted using nonlinear least-squares regression following Jassby and Platt (1976)[33]:

$$P^B = P^B_{max} \times \tanh(\alpha^B \times I / P^B_{max}) \quad (1)$$

where P^B (µg C µg $Chla^{-1}$ h^{-1}) is the chlorophyll-normalized photosynthetic rate, P^B_{max} (µg C µg $Chla^{-1}$ h^{-1}) is the maximum chlorophyll-normalized photosynthetic rate, α^B (µg C µg $Chla^{-1}$ h^{-1} µE^{-1} m^2 s) is the slope of the initial, linear light-limited part of the photosynthesis-irradiance curve, and I (µE m^{-2} s^{-1}) is photosynthetically active radiation. The fitted curves yielded estimates of P^B_{max} and α^B, which were subsequently used to calculate photosynthetic rates under in situ light conditions (see Data analysis).

Respiration measurements

Community respiration (CR) was measured from dissolved oxygen consumption in unfiltered water samples during 48-h dark bottle incubations. Samples were incubated in a temperature-controlled darkroom maintained at the in situ surface water temperature measured during sampling. Water collected from each depth was transferred into triplicate 40 mL serum vials, which were carefully sealed without headspace or air bubbles. Dissolved oxygen concentrations were measured periodically using a Witrox oxygen optode system (Loligo Systems).

All incubations exhibited linear dissolved oxygen declines over time, and respiration rates were calculated from the slope of the regression between dissolved oxygen concentration and incubation duration. The measured CR rates were subsequently used to reconstruct the vertical profile of CR and calculate depth-integrated CR (see Data analysis).

Data analysis

To reconstruct the underwater light field, incident solar radiation at 5-min intervals was obtained from the MesoWest weather stations FW7828 Edenton and GW4330 Edenton, located approximately 20 km and 8 km from the study site, respectively. Solar radiation (W m^{-2}) was converted to photosynthetically active radiation (μE m^{-2} s^{-1}) using a conversion factor of 2.04[34]. The vertical light attenuation coefficient (K_d) was determined from the regression of the natural logarithm of measured photosynthetically active radiation against depth. Light at depth was then estimated following Kirk (1983)[35]:

$$I_z = I_0 e^{-K_d z} \quad (2)$$

where I_z (μE m^{-2} s^{-1}) is the irradiance at depth z (m), I_0 (μE m^{-2} s^{-1}) is incident irradiance at the water surface, and K_d is the vertical light attenuation coefficient.

Depth-specific chlorophyll-normalized photosynthetic rates (P^B) was first calculated by combining the fitted parameters (P^B_{max} and α^B) with the modeled underwater light field using Equation (1). Volumetric GPP was then calculated by multiplying P^B by the chlorophyll *a* concentration at each depth. Daily GPP was calculated for each depth by integrating the volumetric GPP over the daylight period. Depth-integrated GPP was then calculated by integrating the resulting depth-specific daily GPP throughout the water column using trapezoidal integration.

To estimate the vertical profile of CR, measured rates from the surface, Secchi depth, and twice the Secchi depth were linearly interpolated between sampling depths. For depths deeper than twice the Secchi depth, CR was assumed to remain constant and equal to the value measured at twice the Secchi depth. Depth-integrated CR was then calculated by integrating the depth-specific CR throughout the water column using trapezoidal integration.

Carbon-based GPP derived from ^{14}C uptake experiments was converted to oxygen equivalents using a photosynthetic quotient of 1.25[36], whereas CR was expressed directly as oxygen consumption based on dissolved oxygen decline. Depth-integrated NCP was calculated as the difference between depth-integrated GPP and depth-integrated CR.

The uncertainty of depth-integrated NCP was calculated as the square root of the sum of the variances of depth-integrated GPP and CR, assuming that the two sources of uncertainty were independent. For each sampling date, GPP uncertainty was quantified using bootstrap resampling of the photosynthesis-irradiance curve. A total of 2000 bootstrap photosynthesis-irradiance curves were generated by resampling residuals from the original fitted photosynthesis-irradiance relationship with replacement and adding the resampled residuals to the corresponding fitted photosynthesis rates. For each bootstrap iteration, the photosynthesis-irradiance relationship was

refitted using the original photosynthetically active radiation values paired with the bootstrap-generated photosynthesis rates. Each refitted bootstrap curve was used to calculate a complete depth profile of daily GPP. Each of the 2000 GPP profiles was then depth-integrated independently using trapezoidal integration, producing 2000 depth-integrated GPP estimates for each sampling date. The standard deviation of the 2000 depth-integrated GPP was used to quantify uncertainty in depth-integrated GPP. CR uncertainty was propagated using the standard error of the respiration rate estimated from the dissolved oxygen-incubation duration regression at each measured depth. For each measured CR value, a depth-weighting coefficient was calculated by integrating the contribution of that measured value to the interpolated CR profile using trapezoidal integration. Specifically, the weighting assigned to the surface CR decreased linearly from one at the surface to zero at the Secchi depth, the weighting assigned to the CR measured at the Secchi depth increased linearly from zero at the surface to one at the Secchi depth and then decreased linearly to zero at twice the Secchi depth, and the weighting assigned to the CR measured at twice the Secchi depth increased linearly from zero at the Secchi depth (or from zero at the surface if no measurement existed at the Secchi depth) to one at twice the Secchi depth and remained at one below twice the Secchi depth. The variance of each measured CR was then calculated as the squared depth-weighting coefficient multiplied by the squared regression-derived standard error. These variances were summed to obtain the total variance, and the square root of the total variance was reported as the standard error of depth-integrated CR.

One-way analysis of variance (ANOVA) was conducted using the "aov" function in the R package *stats* to test for differences in measured variables across groups. Prior to statistical analysis, response variables were log transformed to improve normality and stabilize variance. When the ANOVA indicated a significant effect ($\alpha = 0.05$), Tukey's honestly significant difference (HSD)

post hoc tests were performed using the "TukeyHSD" function in the R package *stats* to identify significant pairwise differences.

References

1. Leech, D. M., Ensign, S. H., & Piehler., M. F. Spatiotemporal patterns in the export of dissolved organic carbon and chromophoric dissolved organic matter from a coastal, blackwater river. *Aquatic Sciences* 78, 823-836 (2016).
2. Moore, S. et al. Deep instability of deforested tropical peatlands revealed by fluvial organic carbon fluxes. *Nature* 493(7434), 660-663 (2013).
3. Raymond P. A., & Spencer., R. G. M. Riverine DOM. In: Hansell, D. A., and C. A. Carlson (Eds.). 2014. *Biogeochemistry of marine dissolved organic matter*. Academic Press, Bulrlington, pp 509-533 (2015).
4. Williamson, J. L. et al. Landscape controls on riverine export of dissolved organic carbon from Great Britain. *Biogeochemistry* 164(1), 163-184 (2023).
5. Soares, A. R., Kritzberg, E. S., Custelcean, I., & Berggren., M. Bacterioplankton responses to increased organic carbon and nutrient loading in a boreal estuary—separate and interactive effects on growth and respiration. *Microbial Ecology* 76(1), 144-155 (2018).
6. Smith, S. V., & Hollibaugh., J. T. Coastal metabolism and the oceanic organic carbon balance. *Reviews of Geophysics* 31(1), 75-89 (1993).
7. Caffrey, J. M. Factors controlling net ecosystem metabolism in US estuaries. *Estuaries* 27(1), 90-101 (2004).
8. Russell, M. J., & Montagna., P. A. Spatial and temporal variability and drivers of net ecosystem metabolism in western Gulf of Mexico estuaries. *Estuaries and Coasts*, 30(1), 137-153 (2007).

9. Bordin, L. H., da Costa Machado, E., Mendes, C. R. B., Fernandes, E. H. L., & de Camargo M. G. Total ecosystem metabolism variability in a subtropical lagoonal estuary channel-site. *Estuaries and Coasts* 47(1), 276-291 (2024).

10. Flotemersch, J. E. et al. Distribution and characteristics of blackwater rivers and streams of the contiguous United States. *Water Resources Research* 60(2), e2023WR035529 (2024).

11. Stanley, D. W., & Hobble., J. E. Nitrogen recycling in a North Carolina coastal river[1]. *Limnology and Oceanography* 26(1), 30-42 (1981).

12. Pierce, E. et al. Unprecedented toxic blooms of *Microcystis* spp. in 2019 in the Chowan River, North Carolina. *Harmful Algae* 140, 102747 (2024).

13. Wallace, R. B., & Gobler., C. J. The role of algal blooms and community respiration in controlling the temporal and spatial dynamics of hypoxia and acidification in eutrophic estuaries. *Marine Pollution Bulletin* 172, 112908 (2021).

14. NCDEQ. Chowan River Basin Water Resources Plan. Raleigh, NC: North Carolina Department of Environmental Quality (2021).

15. Gomez-Castillo, A. P., Panton, A., & Purdie, D. A. Temporal variability of phytoplankton biomass and net community production in a macrotidal temperate estuary. *Estuarine, Coastal and Shelf Science* 280, 108182 (2023).

16. Arriola, J. M. et al. Ecosystem metabolic rates estimated from diel oxygen measurements in two subtropical estuaries. *Estuaries and Coasts* 48(6), 155 (2025).

17. Gomez Castillo, A. P. Identification of seasonal and interannual drivers of primary production in two temperate estuaries using high-frequency environmental data (Doctoral dissertation, University of Southampton) (2022).

18. Cai, W. J., & Wang., Y. The chemistry, fluxes, and sources of carbon dioxide in the estuarine waters of the Satilla and Altamaha Rivers, Georgia. *Limnology and Oceanography* 43(4), 657-668 (1998).

19. Cai, W. J., Pomeroy, L. R., Moran, M. A., & Wang., Y. Oxygen and carbon dioxide mass balance for the estuarine-intertidal marsh complex of five rivers in the southeastern US. *Limnology and Oceanography* 44(3), 639-649 (1999).

20. Cai, W. J. Estuarine and coastal ocean carbon paradox: CO_2 sinks or sites of terrestrial carbon incineration?. *Annual Review of Marine Science* 3(1), 123-145 (2011).

21. Duarte, C. M., & Prairie, Y. T. Prevalence of heterotrophy and atmospheric CO_2 emissions from aquatic ecosystems. *Ecosystems* 8, 862-870 (2005).

22. Hopkinson, C. S., & Smith., E. M. *Estuarine respiration: an overview of benthic, pelagic, and whole system respiration*. In: del Giorgio, P. A., & Williams, P. J. le B., (eds.), Respiration in Aquatic Ecosystems. Oxford University Press. Oxford, NY, pp. 122-146 (2005).

23. Preen, K., & Kirchman., D. L. Microbial respiration and production in the Delaware Estuary. *Aquatic Microbial Ecology* 37(2), 109-119 (2004).

24. Murrell, M. C. et al. Seasonal oxygen dynamics in a warm temperate estuary: effects of hydrologic variability on measurements of primary production, respiration, and net metabolism. *Estuaries and Coasts* 41(3), 690-707 (2018).

25. Wang, S. R., Di Iorio, D., Cai, W. J., & Hopkinson., C. S. Inorganic carbon and oxygen dynamics in a marsh-dominated estuary. *Limnology and Oceanography* 63(1), 47-71 (2018).

26. Ensign, S. H., Leech, D. M., & Piehler, M. F. Effects of nutrients and zooplankton on an estuary's phytoplankton: inferences from a synthesis of 30 years of data. *Ecosphere* 5(7), 1-25 (2014).

27. Helms, J. R. et al. Loss of optical and molecular indicators of terrigenous dissolved organic matter during long-term photobleaching. *Aquatic Sciences* 76(3), 353-373 (2014).

28. Preisendorfer, R. W. Secchi disk science: Visual optics of natural waters[1]. *Limnology and Oceanography* 31(5), 909-926 (1986).

29. Peierls, B. L., Hall, N. S., & Paerl., H. W. Non-monotonic responses of phytoplankton biomass accumulation to hydrologic variability: a comparison of two coastal plain North Carolina estuaries. *Estuaries and Coasts* 35, 1376-1392 (2012).

30. Vonk, J. E. et al. Biodegradability of dissolved organic carbon in permafrost soils and aquatic systems: a meta-analysis. *Biogeosciences* 12(23), 6915-6930 (2015).

31. Pinckney, J. L., Paerl, H. W., Harrington, M. B., & Howe., K. E. Annual cycles of phytoplankton community-structure and bloom dynamics in the Neuse River Estuary, North Carolina. *Marine Biology* 131, 371-381 (1998).

32. Lewis, M. R., & Smith., J. C. A small volume, short-incubation-time method for measurement of photosynthesis as a function of incident irradiance. *Marine Ecology Progress Series. Oldendorf* 13(1), 99-102 (1983).

33. Jassby, A. D., & Platt., T. Mathematical formulation of the relationship between photosynthesis and light for phytoplankton. *Limnology and Oceanography* 21(4), 540-547 (1976).

34. Fisher, T. R., Gustafson, A. B., Radcliffe, G. M., Sundberg, K. L., & Stevenson., J. C. A long-term record of photosynthetically available radiation (PAR) and total solar energy at 38.6 N, 78.2 W. *Estuaries* 26, 1450-1460 (2003).

35. Kirk, J. T. *Light and photosynthesis in aquatic ecosystems*. Cambridge University Press (1983).

36. Descy, J. P., Servais, P., Smitz, J. S., Billen, G., & Everbecq., E. Phytoplankton biomass and production in the River Meuse (Belgium). *Water Research* 21(12), 1557-1566 (1987).

Acknowledgements

We appreciate the technical assistance of Mary Kate Rinderle, Jeremy Braddy, Randall Sloup, Maxfield Palmer, Chesney Thompson, Lily Goerlitz, Jack Cheshire, Lindsay Yue, Ashlee Somol. This work was supported by the North Carolina Division of Marine Fisheries Commercial Fishing Fund (grant number CW19144), North Carolina Policy Collaboratory (grant number 390), the Andrew Marion Blackmon Fund Fellowship, and EMES Dissertation Completion Fellowship.

Author contributions

M.C. conceived the idea, wrote the manuscript, collected and analyzed the data. N.H. reviewed and edited the manuscript.

Data availability

The data that support the findings of this study are available at https://doi.org/10.15139/S3/CBILLE.

Competing interests

The authors declare no competing interests.